Digest Journal of Nanomaterials and Biostructures Vol. 19, No. 4, October-December 2024, p. 1605-1615

Polyvinyl alcohol and alginate bio-composite film containing titanium dioxide nanotubes for skin injury repair

Z. Huang[a], X. Liu[b], Y. Han[c], L. Li[d], W. Song[a,*], M. Yusoff[e], N. A. Roslan[f], M. H. Razali[f,g]

[a]*Department of Plastic Surgery, Yixing Medical Cosmetology Hospital of Xi'an, Xi'an, 710003, China.*
[b]*Department of Plastic Surgery, Mebel Medical Cosmetology Hospital of Changzhou, Changzhou, 213001, China.*
[c]*Department of Burns and Plastic Surgery, Xi'an Central Hospital, Xi'an, 710005, China.*
[d]*Department of Plastic Surgery, Yueyang Central Hospital, Yueyang, 414020, China.*
[e]*Faculty of Bioengineering and Technology, Universiti Malaysia Kelantan, 17600 Jeli, Kelantan, Malaysia.*
[f]*Faculty of Science and Marine Environment, Universiti Malaysia Terengganu, 21030 Kuala Nerus, Terengganu, Malaysia*
[g]*Advanced Materials Research Group, Faculty of Science and Marine Environment, Universiti Malaysia Terengganu, 21030 Kuala Nerus, Terengganu, Malaysia*

This study explores the potential of polyvinyl alcohol (PVA) and alginate (SA) blend polymer films with embedded titanium dioxide nanotubes (TiO_2NT) for wound healing applications. The nanocomposite film (PVA+SA@TiO_2NT) was fabricated via a simple solvent casting process. The synergistic interaction between PVA and alginate significantly enhanced the film's stability in aqueous environments without compromising its weight. After 24 hours of immersion, the film exhibited a substantial swelling capacity (836±6%) and good WVTR ((282±4%). Scanning electron microscopy (SEM) revealed the formation of a smooth and random pore structure within the film. Fourier-transform infrared spectroscopy (FTIR) confirmed the successful formation of hydrogen bonds between PVA and alginate, along with the presence of Ti-O bonds, indicating successful incorporation of TiO_2NT into the PVA+SA matrix. X-ray diffraction (XRD) analysis further corroborated the presence of TiO_2NT. In vitro biocompatibility studies demonstrated the non-cytotoxic nature of the PVA+SA@TiO_2NT bio-composite film. Additionally, in vitro wound healing studies suggest its potential as a promising biomaterial for wound dressing applications. These findings warrant further investigation to elucidate the complete mechanisms of action and optimize the nanocomposite's properties for clinical translation.

(Received June 26, 2024; Accepted October 23, 2024)

Keywords: Biopolymers, Nanomaterials, Metal oxide, Tissue engineering

1. Introduction

Tissue engineering offers a groundbreaking approach to create functional tissue by manipulating biomechanical factors in a controlled environment. Within this "triad," the building blocks for new tissue are from cells, and biomolecules serve to enhance or supplement the healing process. Although the skin, the body's largest organ, possesses some inherent self-regenerative capacity, extensive injuries and chronic wounds significantly impede this process [1]. Current clinical approaches for skin repair often fall short in achieving rapid wound healing, minimizing

* Corresponding author: 13389227732m@sina.cn
https://doi.org/10.15251/DJNB.2024.194.1605

infection risk, and effectively managing pain. While numerous conventional wound treatments exist, their limitations necessitate the exploration of alternative, more optimal strategies. An ideal wound dressing system should exhibit both antibacterial and antimicrobial properties to combat infection. Bacterial infiltration of the wound site during infection releases compounds that hinder the immune system's ability to clear these pathogens, thereby prolonging healing [2].

Biodegradability, biocompatibility, and non-toxicity are crucial properties. In addition, moist conditions are well-established enhance the healing by supporting angiogenesis (blood vessel formation), collagen production, and minimizing tissue adherence, consequently reducing pain and scab formation [3]. Furthermore, an optimal dressing should effectively absorb wound exudates while facilitating gas exchange between the injured tissue and the surrounding environment. Oxygen acting as critical role in cell growth and blood vessel formation, highlighting the importance of gas permeability [4,5]. Finally, a cost-effective approach is essential for wider clinical adoption. Film wound dressings, compared to other scaffold types like porous scaffolds, hydrogels, or nanofibers, offer specific advantages for wound healing. Film dressings provide a high potential structure for skin repair challenges. Additionally, fabrication of film is relatively straightforward, allowing for immediate application to various wound types.

Polymer films have emerged as a versatile tool in various medical fields, demonstrating utility in treating burns, trauma, radiation injuries, surgical wounds, and chronic conditions like diabetes, obesity-related issues (including pressure ulcers), and delayed wound healing [6]. Their potential extends beyond wound care, offering promising advancements in diagnostic tools, therapeutic approaches, and treatment protocols [7]. The vast application landscape of polymer films is driven by the immense diversity of polymers available. These materials offer exceptional fabrication flexibility, allowing for intricate shapes and structures, coupled with a broad spectrum of compositions and properties. However, a significant limitation of some polymers lies in their inherent flexibility and fragility, which can render them unsuitable for applications requiring high mechanical strength, such as surgical implants [8]. To address these limitations and create polymer films with enhanced properties, researchers often employ blend polymers. Blending polymers has been shown to significantly impact their physical properties, including mechanical behavior, thermal stability, and electrical conductivity [9]. The careful selection and thorough integration of a guest material with the host polymer can influence either the amorphous or crystalline regions, leading to tailored properties.

Among the polymers with high biocompatibility and biodegradability suitable for biomedical applications is alginate [10]. However, its inherent rigidity and fragility limit its processing capabilities to primarily spherical shapes. Chemically, categorised as is a binary and unbranched copolymer, alginate composed of β-D-mannuronic acid (M) residues linked glycosidic [11]. Derived from brown marine algae, sodium alginate holds value as stabilizer, gelling agent and forming viscous solutions upon dissolution in water [12, 13]. While, polyvinyl alcohol (PVA), a well-established hydrophilic polymer, offers a compelling material for biomedical applications due to non-carcinogenicity, and biodegradability [14,15]. These make PVA a suitable candidate as a co-polymer to alginate for bio-implants, and wound dressings. Notably, PVA's linear structure allows for crosslinking via various methods like irradiation, thermal cycling, and chemical reactions. Additionally, its biological inertness, biocompatibility, and transparency further contribute to its widespread use in wound healing applications [16].

Recent research suggests that incorporating metal oxides into polymers can significantly impact wound healing such as titanium dioxide (TiO_2) nanoparticles [17]. The nanoparticle-released titanium ions show strong antibacterial activity [18]. The initial stage of wound healing, hemostasis and inflammation, requires blood clotting and elimination of microbial invaders to facilitate fibroblast and keratinocyte proliferation. Beyond its antimicrobial properties, TiO_2 can act as a reinforcing agent, providing substantial mechanical strength to support cell growth [19]. Moreover, studies have shown that TiO_2 promotes wound healing [20,21]. The low toxicity of TiO_2 further strengthens its candidacy for biomedical applications, as evidenced by its approval and widely used commercially [22].

In this research, hydrothermally synthesised TiO_2 nanotubes was incorporated into polyvinyl alcohol and sodium alginate to produce bio-composite film for ideal wound dressing application in the future. The film was produced using solvent casting method. The structural,

antibacterial and other biological properties of PVA+SA@TiO_2NT bio-composite film were investigated for wound healing application.

2. Materials and methods

2.1. Materials

Biopolymer of sodium alginate (SA), polyvinyl alcohol (PVA) and chemicals for cell culture were purchased from Sigma-Aldrich. Titanium dioxide (TiO_2), sodium hydroxide (NaOH), and acid hydrochloric (HCl), 99.5% trace metals basis were purchased from Merck. Each of the materials and other chemical solvent were standard analytical grade and were utilized in its original state without any modifications.

2.2. Preparation of TiO_2 Nanotubes

For thirty minutes, TiO_2 powder (2.0 g) was continuously stirred in 10 M NaOH (100 mL). After 30 minutes of sonication in a sonicator bath, the mixture was continuously stirred at 500 rpm for an additional 30 minutes. The mixture was then put into a Teflon vessel and autoclaved for 24 hours at 150 °C to undergo hydrothermal treatment. After the reaction was finished, the white solid precipitate was gathered and mixed with 0.1 M HCL in order to wash it until its pH was reached 7. After washing, the washing solution was added distilled water, and it was then dried in an oven for 24 hours at 80 °C. To produce TiO_2 nanotubes, the dried sample was then calcined for two hours at 400 °C. respectively.

2.3. Preparation of *of PVA+SA@TiO_2NT bio-composite film*

100 ml of distilled water was used to dissolve each 4 g of PVA and SA polymer, which was then stirred at 50 °C. 0.1 g of TiO_2 nanotubes was added and stirred mixture until all completely dissolved. To create film, the solution was dried in an oven at 50 °C for 24 hours. The same steps were taken to prepare the pure PVA+SA film.

2.4. Characterization

Fourier transform infrared (FTIR) spectroscopy was used to analyze the synthesized sample and fabricated films at a wavenumber range of 4000-400 cm^{-1}. The x-ray diffraction (XRD) pattern patterns were collected using a Rigaku Miniflex (II) X-ray diffractometer wide-angle region from 10-80°. The examination of the samples' surface morphology was conducted through the utilization of JOEL JSM 6360 LA scanning electron microscopy (SEM). An assessment of the sample's thermogravimetric properties was carried out using a Perkin Elmer STA 8000 thermogravimetric analyzer from 37°C to 900°C at a rate of 10°/min in a nitrogen atmosphere.

2.5. Swelling study

PVA+SA@TiO_2 film was cut to a similar size (measuring 20 mm x 20 mm) and weighed (Wd). The samples were then placed into distilled water at a temperature of 37°C. After 24 hours, the samples were removed from and any water on their surface was quickly wiped off. The fully enlarged films were then weighed (Ws) and the swelling percentage (%) was calculated using the following Equation 1;

$$\text{Swelling (\%)} = \frac{(W_s - W_d)}{W_d} \text{ X } 100 \quad (1)$$

2.6. Water vapor transmission rates

A modified version of the ASTM International standard method was employed to determine the water vapor transmission rate (WVTR). The films were placed in a desiccator at 25 °C and 50 ± 5% relative humidity. They were secured over the circular opening of a permeation bottle (diameter = 1.5 cm, height = 5.0 cm) with an effective transfer area (A = 1.33 cm^2). The rate of mass change (m) in these water-filled permeation bottles, measured over a 24-hour exposure period, was then used to calculate the WVTR using Equation 2 as follows:

$$WVTR = (m/A\ \Delta t) \quad (2)$$

where $m/\Delta t$ is the water gain per unit time of transfer inhibition and A is the area exposed to water transfer (m^2).

2.7. Cytotoxicity and biocompatibility study

An assessment was conducted on the cytocompatibility and proliferation of 3T3 mouse fibroblast cells. After being incubated for 72 hours, the cell viability in contact with the biofilm samples was evaluated using an acridine orange/propidium iodide (AO/PI) staining technique (Sigma Aldrich, USA), which was then visualised under an Olympus IX73-FL-CCD light microscope. The negative control was Dulbecco's Modified Eagle Medium (DMEM) culture medium without film samples. An MTT (3-(4,5-dimethylthiazol-2-yl)-2,5-diphenyltetrazolium bromide) test (Thermo Fisher Scientific, USA) was used to measure the proliferation of cells. In short, each well containing film samples or the negative control (sample-free) received 50 µL of MTT solution. A microplate reader (Multiskan Ascent 96/384, USA) was used to measure the absorbance. Using a calibration curve created with grown 3T3 mouse fibroblast cells, absorbance data were translated to cell counts.

2.8. In vitro wound healing studies

Wound healing experiments in vitro were carried out employing a scratch wound assay, as detailed in a previous publication [23]. The scratch wound assay represents a widely recognized technique for assessing the migratory potential of fibroblasts and their capacity to seal wounds, a critical aspect in the process of wound healing [24, 25]. 3T3 fibroblast cells were cultured in a 24-well plate for 24 hours to establish a cell monolayer with 80%–90% confluence. Following this, a serum-free media supplemented with mitomycin C (5 g/mL) was applied to the cells for 12 hours to impede cell proliferation, succeeded by a thorough wash to eliminate any remaining mitomycin C. Linear wounds were then generated in the cell monolayers using a micropipette tip, resulting in areas devoid of cells. The scratched wells underwent three washes with PBS to get rid of any floating or detached cells. The closure rate of the wounds was observed and recorded 24 hours post-scratching using an inverted microscope, with corresponding images captured.

3. Results and discussions

Fig. 1(a) displays the FTIR spectrum of the synthesized TiO_2NT powder, where a distinct peak at 439 cm^{-1} indicates the Ti-O stretching vibration, a typical feature of TiO_2. The FTIR spectrum of the pure PVA+SA blend film (Fig. 1(b)) shows a pronounced, broad peak at 3311 cm^{-1}, which is attributed to O-H stretching vibrations. This broad peak reflects the formation of hydrogen bonds between the hydroxyl groups (-OH) of SA and PVA [26]. The hydroxyl groups present in both PVA and SA facilitate intermolecular hydrogen bonding (O-H···O), as reported in earlier studies [27,28]. Moreover, intramolecular hydrogen bonding can occur within each polymer, with interactions such as O-H···O-C (between two hydroxyl groups) and C-H···O-C (between a hydroxyl and a carboxylic acid group). When PVA and SA are dissolved and mixed in water, the sodium carboxylate groups (-COONa) in SA transform into negatively charged carboxylic acid groups (-COO-). These hydroxyl and carboxylate groups may form hydrogen bonds with each other [29,30]. This specific hydrogen bonding, due to its proximity to the broad O-H band, would appear as a broadened peak centered around 3311 cm^{-1} in the spectrum. The peaks at 2915 cm^{-1} and 2851 cm^{-1} correspond to the asymmetric stretching vibrations of C-H bonds [31]. The strong, sharp peaks at 1601 cm^{-1} and 1409 cm^{-1} are due to the symmetric and antisymmetric stretching vibrations of the carbonyl groups (C=O) in PVA and SA, respectively [32]. The bands at 1321 cm^{-1} and 1258 cm^{-1} are attributed to the stretching vibrations of the $-CH_2$ and -CH groups, respectively [33]. The peaks at 1081 cm^{-1} and 1021 cm^{-1} are due to the stretching vibrations of the C-O-C groups within the sugar structure and pyranose ring, respectively [34–36]. The PVA+SA@TiO_2NT composite exhibited a similar FTIR spectrum, with additional peaks at 836 cm^{-1}, 609 cm^{-1}, and 944 cm^{-1} (Fig. 1(c)). In the PVA+SA@TiO_2NT bio-composite film, the peaks below 1000 cm^{-1} are related to metal oxide bonds and interactions between metals, including Ti-O, Ti-C, and Ti-Ti [37]. Due to the interaction

between PVA+SA and TiO_2NT as a filler, the functional group bands for the PVA+SA@TiO_2NT bio-composite film are often slightly shifted compared to those in PVA+SA.

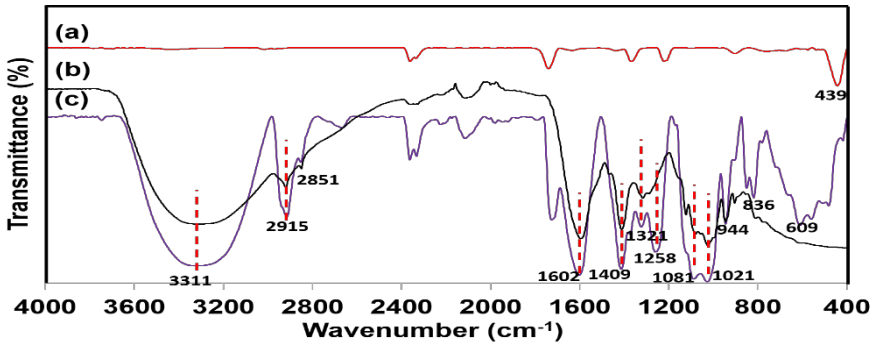

Fig. 1. FTIR spectra of (a) TiO_2NT powder, (b) PVA+SA and (c) PVA+SA@TiO_2NT bio-composite film.

Fig. 2 displays the X-ray diffraction (XRD) patterns of TiO_2NT powder, PVA+SA blended polymer, and the PVA+SA@TiO_2NT bio-composite film. The TiO_2NT pattern assigned to anatase TiO_2 (Fig. 1(a). These findings are consistent with previous reports [38,39]. The pure PVA+SA blended polymer film shows a broad, low-intensity peak at $2\theta = 19.6°$, corresponding to the (110) lattice plane and indicating an amorphous state. Other researchers have noted that PVA+SA's crystallinity is probably decreased during the mixing procedure [40, 41]. This theory is supported by the PVA+SA film's broad peak and low intensity in Figure 2(b), resulted from formation of intermolecular hydrogen bonds between PVA and SA macromolecules during mixing [42]. The presence of these hydrogen bonds is confirmed by the broad peaks observed around 3300 cm^{-1} in FTIR analysis. Interestingly, the bio-composite film after incorporating TiO_2NT still displays peaks around 19°, but with increased intensity, suggesting enhanced crystallinity in the PVA+SA@TiO_2NT bio-composite film. Furthermore, the characteristic peaks of anatase TiO_2 appear alongside a single peak corresponding to rutile TiO_2 at 28° [43]. This mixed-phase TiO_2 and the highly crystalline nature of the PVA+SA@TiO_2NT bio-composite film may contribute to generation of reactive oxygen species (ROS), potentially improving the film's ability to promote skin repair.

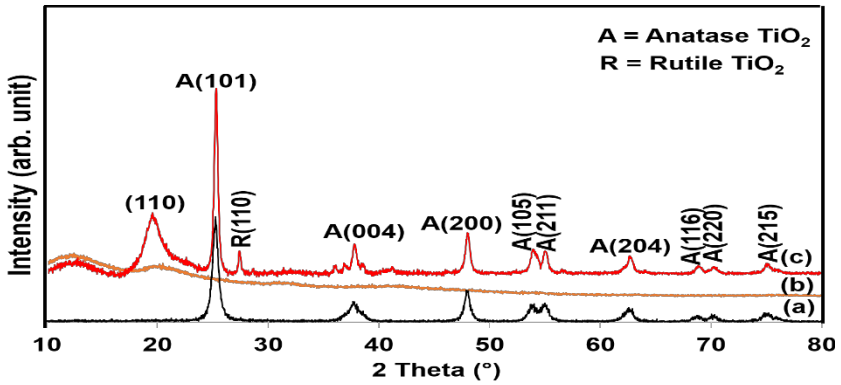

Fig. 2. XRD pattern of (a) TiO_2NT powder, (b) PVA+SA and (c) PVA+SA@TiO_2NT bio-composite film.

SEM analysis (Fig. 3(a) reveals the presence of agglomerated TiO_2NT. This agglomeration likely occurs during the calcination process employed in TiO_2NT preparation. As a well-established phenomenon, the heating process can promote particle agglomeration to minimize surface energy [44]. The bundled nature of the TiO_2NT hinders accurate measurement of their diameter and length.

Nevertheless, the synthesized TiO_2NT exhibit an estimated diameter of approximately 80 nm. Pure PVA+SA blended polymer and PVA+SA@TiO_2NT bio-composite films display smooth surface (Fig 3(b), and roughened surface with noticeable grain formation (Fig. 3(c), respectively. This phenomenon can be attributed to the attractive forces arising between the hydrophilic interphase surrounding the TiO_2NT and the polymer matrix. These interactions lead to the formation of grains, which become evident on the bio-composite surface.

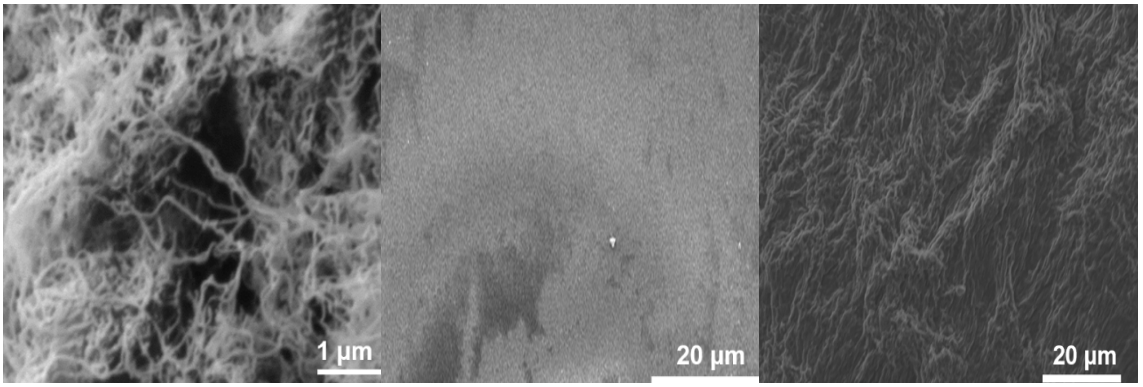

Fig. 3. SEM micrographs of (a) TiO_2NT powder, (b) PVA+SA and (c) PVA+SA@TiO_2NT bio-composite film.

Thermal characteristics of synthesized TiO_2NT powder and the PVA+SA@TiO_2NT bio-composite film were shown in Fig. 4. The TGA profile revealed excellent thermal stability for the TiO_2NT powder, with a minimal weight loss of only 4.58% observed between 30 °C and 900 °C. In contrast, the bio-nanocomposite film exhibited significantly lower thermal stability, undergoing a total weight loss of 81.28%. Approximately 12% weight loss below 200°C, likely due to the evaporation of moisture adsorbed within the sample. This was followed by two distinct stages of substantial weight loss: 49.82% between 200°C and 290°C, and 29.83% between 290°C and 890°C. These significant losses due to degradation of the polymeric components (PVA and SA) within the nanocomposite [45]. Interestingly, previous studies have reported contrasting observations [46], suggesting a positive effect in this study. Further investigation is warranted to reconcile these discrepancies and elucidate the specific interactions between TiO_2 and the PVA+SA matrix in this bio-composite system.

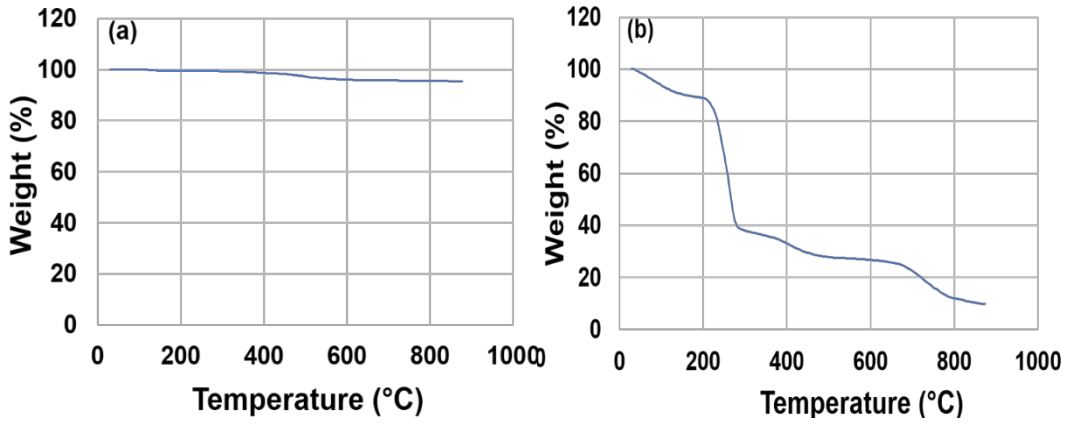

Fig. 4. TGA thermograms of (a) TiO_2NT powder and (b) PVA+SA@TiO_2NT bio-composite film.

The PVA+SA@TiO_2NT demonstrated significantly higher swelling (836 ± 6%) compared to pure PVA+SA film (675±8%). The incorporation of TiO_2NT promoting greater water absorption and facilitating the adsorption of TiO_2 molecules within the film structure. Additionally, the hydrophilic nature of TiO_2 contributes to the enhanced swelling properties of PVA+SA@TiO_2NT. This improved water absorption capability is crucial for maintaining a dry wound environment and preventing airborne infections. However, PVA+SA@TiO_2NT bio-composite film exhibited a slight decrease in WVTR to 282±4% instead of 348±8% for pure PVA+SA film because the formation of nanoparticle agglomerates on the surface of the PVA+SA@TiO_2NT biocomposite film.

In addition, the bio-composite film made of PVA+SA@TiO_2NT is extremely biocompatible with 3T3 fibroblast cells and non-toxic. The cells spread out more as the culture period rose, and after three days, the cells spread out widely, indicating that they were amazingly cultivating as well as thriving towards that bio-composite surface. Figs. 9(a) and 9(b) show the cell viability following their treatment with PVA+SA/TiO_2NT and PVA+SA films, respectively. The amount of proliferation detected is nearly identical to the reported cell viability. Following a 72-hour exposure to the PVA+SA@TiO_2NT bio-composite film and pure PVA+SA film, the amount were 120,400 cells/well and 75,228 cells/well, respectively. The film shows good biocompatibility towards cells, indicating that the PVA+SA blend polymer is not hazardous. Given that the PVA+SA@TiO_2NT bio-composite film in this study showed improved cell survival and proliferation, it is interesting to note that the integration of TiO_2NT is non-toxic and appropriate for cell.

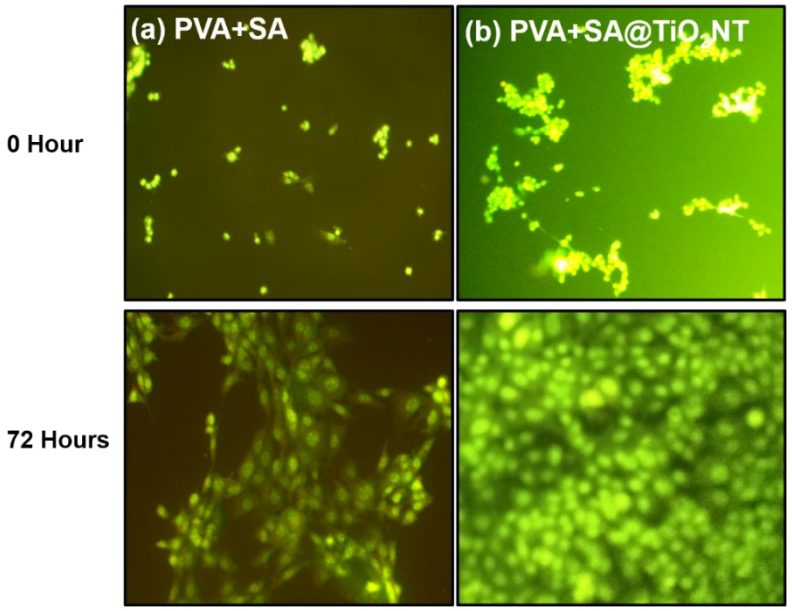

Fig. 5. Fluorescence microscope images of the cell viability on the (a) pure PVA+SA and (b) PVA+SA@TiO_2NT bio-composite films after incubated in the media for 72 h.

The scratch assay was studied, which is a preferred method for assessing the potential of wound dressing application materials. The finding indicated that the number of cells population that migrated in the PVA+SA@TiO_2NT bio-composite film (Fig. 6(a) was relatively faster as compared to the control (Fig. 6(b). The PVA+SA@TiO_2NT film exhibited a better wound closure as significantly increased cell population and migration. These findings indicate that incorporating TiO_2NT into the PVA+SA film positively impacts cell migration. The presence of TiO_2NT promotes the highest rate of cell migration, attributed to its free radical scavenging activity and enhanced antibacterial properties, which help prevent bacterial infection and facilitate wound healing [47,48].

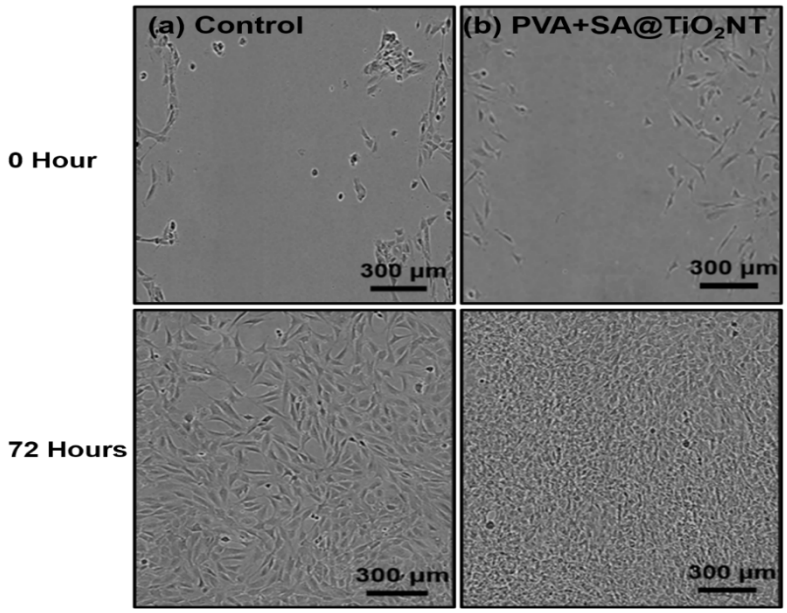

Fig. 6. Illustrations of fibroblast cells moving into a scratch area at 0 and after 72 hours for (a) control sample and in the presence of (b) PVA+SA@TiO_2NT bio-composite film.

4. Conclusion

This study investigated the development of a promising PVA+SA@TiO_2NT bio-composite film for wound healing. FTIR analysis revealed a significant enhancement effect because of TiO_2NT, suggesting strong bonding within PVA+SA components. XRD spectra confirmed the PVA+SA@TiO_2NT is crystalline with anatase and rutile phase TiO_2. SEM micrographs demonstrated the rough surface due to presence of TiO_2NT, a crucial characteristic for promoting wound healing. Rapid fibroblast cell migration on the PVA+SA@TiO_2NT bio-composite film suggesting that the film is a good biomaterial for wound dressing applications.

Acknowledgements

The authors are grateful to Universiti Malaysia Terengganu (UMT) for facilities and Malaysia Ministry of Higher Education for the financial support vote (FRGS/1/2023/STG05/UMT/02/7).

References

[1] Yang, F., Bai, X., Dai, X. and Li, Y., (2021), Regenerative medicine, 16(04), pp.373-390; https://doi.org/10.2217/rme-2020-0066

[2] Holloway, S. and Harding, K.G., (2022), Surgery (Oxford), 40(1), pp.25-32; https://doi.org/10.1016/j.mpsur.2021.11.002

[3] Varaprasad, K., Jayaramudu, T., Kanikireddy, V., Toro, C., Sadiku, E.R., 2020, Carbohydrate polymers, 236, p.116025; https://doi.org/10.1016/j.carbpol.2020.116025

[4] Sheokand, B., Vats, M., Kumar, A., Srivastava, C.M., Bahadur, I., Pathak, S.R., (2023), Journal of Polymer Science, 61(14), pp.1389-1414;

https://doi.org/10.1002/pol.20220734

[5] Kaya, S., Derman, S., (2023), Journal of Faculty of Pharmacy of Ankara University, 47(3), pp.1119-1131; https://doi.org/10.33483/jfpau.1253376

[6] Mh Busra, F., Rajab, N.F., Tabata, Y., Saim, A.B., BH Idrus, R., Chowdhury, S.R., (2019), Journal of tissue engineering and regenerative medicine, 13(5), pp.874-891; https://doi.org/10.1002/term.2842

[7] Bambole, V.; Yakhmi, J.V. (2016), Nanobiomaterials in Soft Tissue Engineering; Elsevier: Amsterdam, The Netherlands, 387-455; https://doi.org/10.1016/B978-0-323-42865-1.00014-3

[8] Mannella, G.A.; Pavia, F.C.; La Carrubba, V.; Brucato, V. (2016), Eur. Polym. J, 79, 176-186; https://doi.org/10.1016/j.eurpolymj.2016.04.025

[9] Aslam, M., Kalyar, M. A., Raza, Z. A. (2018), Polymer Engineering & Science, 58(12), 2119-2132; https://doi.org/10.1002/pen.24855

[10] Hegde, V., Uthappa, U. T., Altalhi, T., Jung, H. Y., Han, S. S., Kurkuri, M. D. (2022), Materials Today Communications, 33, 104813; https://doi.org/10.1016/j.mtcomm.2022.104813

[11] Pawar, S. N., Edgar, K. J. (2012), Biomaterials, 33(11), 3279-3305; https://doi.org/10.1016/j.biomaterials.2012.01.007

[12] Łabowska, M. B., Jankowska, A. M., Michalak, I., Detyna, J., Kulbacka, J. (2020), Advances in Biomedical Research-from COVID to Medical Humanities, 97.

[13] Zia, K. M., Zia, F., Zuber, M., Rehman, S., Ahmad, M. N. (2015), International journal of biological macromolecules, 79, 377-387; https://doi.org/10.1016/j.ijbiomac.2015.04.076

[14] Mbhele, Z. H., Salemane, M. G., Van Sittert, C. G. C. E., Nedeljković, J. M., Djoković, V., Luyt, A. S. (2003), Chemistry of Materials, 15(26), 5019-5024; https://doi.org/10.1021/cm034505a

[15] Jannesari, M., Varshosaz, J., Morshed, M., Zamani, M. (2011), International journal of nanomedicine, 993-1003; https://doi.org/10.2147/IJN.S17595

[16] Kim, J.O., Park, J.K., Kim, J.H., Jin, S.G., Yong, C.S., Li, D.X., Choi, J.Y., Woo, J.S., Yoo, B.K., Lyoo, W.S. Kim, J.A., (2008), International journal of pharmaceutics, 359(1-2), pp.79-86; https://doi.org/10.1016/j.ijpharm.2008.03.021

[17] Su, R., Su, W., Cai, J., Cen, L., Huang, S., Wang, Y. Li, P., (2024), International Journal of Biological Macromolecules, 254, p.127716; https://doi.org/10.1016/j.ijbiomac.2023.127716

[18] Venkataprasanna, K.S., Prakash, J., Vignesh, S., Bharath, G., Venkatesan, M., Banat, F., Sahabudeen, S., Ramachandran, S., Venkatasubbu, G.D., (2020), International journal of biological macromolecules, 143, pp.744-762; https://doi.org/10.1016/j.ijbiomac.2019.10.029

[19] Karthikeyan, K.T., Nithya, A., Jothivenkatachalam, K., (2017), International journal of biological macromolecules, 104, pp.1762-1773; https://doi.org/10.1016/j.ijbiomac.2017.03.121

[20] Prakash, J., Venkataprasanna, K.S.K., Prema, D., Sahabudeen, S.M., Debashree Banita, S. and Venkatasubbu, G.D., (2020), Toxicology Mechanisms and Methods, 30(7), pp.508-525; https://doi.org/10.1080/15376516.2020.1765061

[21] Zhao, J., Li, N., Wang, S., Zhao, X., Wang, J., Yan, J., Ruan, J., Wang,

H., Hong, F., (2010), Journal of Experimental Nanoscience, 5(5), pp.447-462; https://doi.org/10.1080/17458081003628931

[22] Zhu, Z., Cai, H. and Sun, D.W., (2018), Trends in Food Science & Technology, 75, pp.23-35; https://doi.org/10.1016/j.tifs.2018.02.018

[23] Doostan, M., Doostan, M., Mohammadi, P., Khoshnevisan, K., Maleki, H., (2023), International Journal of Biological Macromolecules, 228, pp.506-516; https://doi.org/10.1016/j.ijbiomac.2022.12.228

[24] You, C., Li, Q., Wang, X., Wu, P., Ho, J.K., Jin, R., Zhang, L., Shao, H., Han, C., (2017), Scientific reports, 7(1), p.10489; https://doi.org/10.1038/s41598-017-10481-0

[25] Radstake, W.E., Gautam, K., Van Rompay, C., Vermeesen, R., Tabury, K., Verslegers, M., Baatout, S., Baselet, B., (2023), Biochemistry and Biophysics Reports, 33, p.101423; https://doi.org/10.1016/j.bbrep.2023.101423

[26] Shevchenko, R.V., Eeman, M., Rowshanravan, B., Allan, I.U., Savina, I.N., Illsley, M., Salmon, M., James, S.L., Mikhalovsky, S.V., James, S.E., (2014), Acta biomaterialia, 10(7), pp.3156-3166; https://doi.org/10.1016/j.actbio.2014.03.027

[27] Rahman, N.A.A., Musa, M., Kassim, K., Said, N.R., (2023), Malaysian Journal of Analytical Sciences, 27(2), pp.314-328

[28] Liao, Q., Rong, H., Zhao, M., Luo, H., Chu, Z., Wang, R. (2022), Journal of Hazardous Materials, 422: 126863; https://doi.org/10.1016/j.jhazmat.2021.126863

[29] Ebrahimi, F., Sadeghizadeh, A., Neysan, F., Heydari, M., (2019), Heliyon, 5(11), p.e02941; https://doi.org/10.1016/j.heliyon.2019.e02941

[30]Coleman, M.M., Pehlert, G.J., Painter, P.C., (1996), Macromolecules, 29(21), pp.6820-6831; https://doi.org/10.1021/ma9604045

[31] Wang, T., Zhang, F., Zhao, R., Wang, C., Hu, K., Sun, Y., Politis, C., Shavandi, A., Nie, L., (2020), Designed monomers and polymers, 23(1), pp.118-133; https://doi.org/10.1080/15685551.2020.1804183

[32] Duru Kamaci, U., Peksel, A., (2021), Catalysis Letters, 151, pp.821-831; https://doi.org/10.1007/s10562-020-03339-0

[33] Shehap, A.M., (2008), Egypt. J. Solids, 31(1), pp.75-91; https://doi.org/10.21608/ejs.2008.148824

[34] Tsukada, M., Freddi, G. and Crighton, J.S., (1994), Journal of Polymer Science Part B: Polymer Physics, 32(2), pp.243-248; https://doi.org/10.1002/polb.1994.090320205

[35] Patel, J.P., Xiang, Z.G., Hsu, S.L., Schoch, A.B., Carleen, S.A., Matsumoto, D., (2017), International Journal of Adhesion and Adhesives, 78, pp.256-262; https://doi.org/10.1016/j.ijadhadh.2017.08.006

[36] Patel, J.P., Hsu, S.L., (2018), Journal of Polymer Science Part B: Polymer Physics, 56(8), pp.639-643; https://doi.org/10.1002/polb.24583

[37] Razali, M.H., Noor, A.F.M., Yusoff, M., (2017), Science of Advanced Materials, 9(6), pp.1032-1041; https://doi.org/10.1166/sam.2017.3071

[38] Kanoun, M. B., Ahmed, F., Awada, C., Jonin, C., Brevet, P. F. (2024), International Journal of Hydrogen Energy, 51, 907-913; https://doi.org/10.1016/j.ijhydene.2023.10.244

[39] Razali, M. H., Ismail, N. A., Amin, K. A. M. (2020), International journal of biological macromolecules, 153, 1117-1135;

https://doi.org/10.1016/j.ijbiomac.2019.10.242

[40] Abdelghany, A.M., Menazea, A.A., Ismail, A.M., (2019), Journal of Molecular Structure, 1197, pp.603-609; https://doi.org/10.1016/j.molstruc.2019.07.089

[41] Abdelghany, A.M., Oraby, A.H., Farea, M.O., (2019), Physica B: Condensed Matter, 560, pp.162-173; https://doi.org/10.1016/j.physb.2019.02.029

[42] Li, X., Shu, M., Li, H., Gao, X., Long, S., Hu, T, Wu, C. (2018), RSC Advances, 8(30), 16674-16689; https://doi.org/10.1039/C8RA01302K

[43] Thakur, N., Thakur, N., Kumar, A., Thakur, V. K., Kalia, S., Arya, V. Kyzas, G. Z. (2024), Science of The Total Environment, 169815; https://doi.org/10.1016/j.scitotenv.2023.169815

[44] Shejale, K. P., Krishnapriya, R., Patil, H., Laishram, D., Rawal, P., Sharma, R. K. (2021), Materials Advances, 2(23), 7502-7529; https://doi.org/10.1039/D1MA00942G

[45] Gholamali, I., Yadollahi, M., (2020), International Journal of Biological Macromolecules, 160, pp.724-735; https://doi.org/10.1016/j.ijbiomac.2020.05.232

[46] Mofokeng, J.P., Luyt, A.S., (2015), Polymer Testing, 45, pp.93-100; https://doi.org/10.1016/j.polymertesting.2015.05.007

[47] Kunrath, M. F., Leal, B. F., Hubler, R., de Oliveira, S. D., Teixeira, E. R. (2019), Amb Express, 9(1), 51; https://doi.org/10.1186/s13568-019-0777-6

[48] Lin, Y., Liu, X., Liu, Z., Xu, Y. (2021), Small, 17(39), 2103348; https://doi.org/10.1002/smll.202103348